Inwardly Rectifying Current-Voltage Relationship of Small-Conductance Ca^{2+}-Activated K^+ Channels Rendered by Intracellular Divalent Cation Blockade

Heun Soh and Chul-Seung Park
Department of Life Science, Kwangju Institute of Science and Technology (K-JIST), Kwangju 500–712, Korea

ABSTRACT Small conductance Ca^{2+}-activated K^+ channels (SK_{Ca} channels) are a group of K^+-selective ion channels activated by submicromolar concentrations of intracellular Ca^{2+} independent of membrane voltages. We expressed a cloned SK_{Ca} channel, rSK2, in *Xenopus* oocytes and investigated the effects of intracellular divalent cations on the current-voltage (I-V) relationship of the channels. Both Mg^{2+} and Ca^{2+} reduced the rSK2 channel currents in voltage-dependent manners from the intracellular side and thus rectified the I-V relationship at physiological concentration ranges. The apparent affinity of Mg^{2+} was changed as a function of both transmembrane voltage and intracellular Ca^{2+} concentration. Extracellular K^+ altered the voltage dependence as well as the apparent affinities of Mg^{2+} binding from intracellular side. Thus, the inwardly rectifying I-V relationship of SK_{Ca} channels is likely due to the voltage-dependent blockade of intracellular divalent cations and that the binding site is located within the ion-conducting pathway. Therefore, intracellular Ca^{2+} modulates the permeation characteristics of SK_{Ca} channels by altering the I-V relationship as well as activates the channel by interacting with the gating machinery, calmodulin, and SK_{Ca} channels can be considered as Ca^{2+}-activated inward rectifier K^+ channels.

INTRODUCTION

Small conductance calcium-activated potassium channels (SK_{Ca} channels) play important roles in excitable cells such as neurons in the central nervous system (Vergara et al., 1998). These channels are potassium-selective, voltage-independent, and activated by an increase in the level of intracellular calcium concentration. The activation of SK_{Ca} channels underlies the slow after-hyperpolarization that inhibits neuronal cell firing (Hille, 1992; Vergara et al., 1998). Complementary DNAs (cDNAs) encoding three different isoforms of SK_{Ca} channels were cloned from rat brain, and their electrophysiological characteristics were investigated (Kohler et al., 1996). One of the cloned channels, SK2, is highly sensitive to a bee venom toxin, apamin, whereas SK1 channels are not much affected by the toxin. SK3 channels show an intermediate affinity for the toxin (Kohler et al., 1996; Ishii et al., 1997). Recently, it was shown that channel activation is caused by conformational changes of the channel protein induced by the binding of Ca^{2+} to calmodulin molecules bound constitutively at the intracellular C-terminus (Keen et al., 1999).

Although the activation of SK_{Ca} channels is voltage-independent, both native and the cloned channels show inwardly rectifying current-voltage (I-V) relationships (Lancaster et al., 1991; Kohler et al., 1996; Xia et al., 1998). The I-V relationship is a characteristic of an ion channel governed not only by the properties of ion conduction pore but also by the molecules affecting ion permeation. In the case of inward-rectifier K^+ channels (K_{ir} channels), the inwardly rectifying I-V relationship is due to the blockade of channel currents by intracellular cations such as Mg^{2+} and polyamines (Lu and MacKinnon, 1994; Doupnik et al., 1995; Spassova and Lu, 1998). Magnesium ions block the K_{ir} channel current by binding at a site within the conduction pore from the intracellular side. Because the Mg^{2+} binding site is located within the transmembrane electric field, the binding affinity is dependent upon membrane voltages, and thus the outward currents are blocked more significantly than the inward currents.

In this study, we expressed a cloned rat SK_{Ca} channel, rSK2, and investigated the mechanism of the inwardly rectifying I-V relationship using electrophysiological techniques. We found that the rSK2 channel currents were specifically blocked by intracellular divalent cations such as Ca^{2+} and Mg^{2+} in voltage-dependent manners. The affinity of intracellular Mg^{2+} was dependent on the concentration of intracellular Ca^{2+} and that of extracellular K^+. These results indicated that the voltage-dependent blockade by intracellular divalent cations such as Mg^{2+} and Ca^{2+} underlies the inwardly rectifying I-V relationship of SK_{Ca} channels.

MATERIALS AND METHODS

Expression of rSK2 channels in *Xenopus* oocytes

All electrophysiological experiments were done on rSK2 channels expressed in *Xenopus* oocytes. *Xenopus laevis* (*Xenopus*One, Dexter, MI) was cared for and handled as described previously in accordance with the highest standards of institutional guidelines (Park and MacKinnon, 1995; Ha et al., 2000). The cDNA for rSK2 channel (Kohler et al., 1996) was obtained from Dr. J. P. Adelman (The Vollum Institute, Oregon Health Sciences University, Portland, OR) and subcloned into the pGH expression

Received for publication 27 October 2000 and in final form 5 February 2001.

Address reprint requests to Chul-Seung Park, Ph.D., Department of Life Science, Kwangju Institute of Science and Technology (K-JIST), 1 Oryong-dong, Puk-gu, Kwangju 500–712, Korea. Tel: +82-62-970-2489; Fax: +82-62-970-2484; E-mail: cspark@kjist.ac.kr.

0006-3495/01/05/2207/09 $2.00

vector for high-level expression in *Xenopus* oocytes (Liman et al., 1992). Complementary RNAs for the rSK2 channels were synthesized in vitro from a *Nco*I-linearized plasmid using T7 polymerase (Promega, Madison, WI). Oocytes were injected with approximately 50 ng of RNA and the injected oocytes were incubated at 18°C for 1 to 7 days in ND96 solution containing 5 mM HEPES, 96 mM NaCl, 2 mM KCl, 1.8 mM $CaCl_2$, 1 mM $MgCl_2$, and 50 μg/ml gentamicin, pH 7.6, adjusted with NaOH.

Electrophysiological recordings

Ionic currents carried by rSK2 channels were recorded from patches of oocyte membrane in the inside-out configuration using an Axopatch 200B amplifier (Axon Instruments, Foster City, CA). Patch recordings in the inside-out configuration were made at room temperature (~23°C) 3 to 7 days after injection. Pipettes prepared from thin-walled borosilicate glass (World Precision Instruments, Sarasota, FL) had resistance of 1 to 4 MΩ. Signals were filtered at 1 kHz using a four-pole low-pass Bessel filter, digitized at the rate of 200 samples/ms using Digidata 1200 (Axon Instruments), and stored in a personal computer. PClamp7 software (Axon Instruments) was used to control the amplifier and to acquire the data. For macroscopic current recordings, the membrane was held at 0 mV and ramped from −100 mV to 100 mV over 1 s. In order to ensure that a steady state blockade was achieved throughout the ramp, the current blockade by internal Mg^{2+} was determined using an independent protocol of voltage steps lasting 100 ms. These control experiments gave the same results and therefore validated the use of ramps to accurately measure the current blockade. We observed a variable degree of channel rundown in the absence of any treatment in about 30% of patches. Patches exhibiting severe rundown, in that channel activity was lost within the first minute of recording, were excluded from the analysis.

Recording solutions

Pipette (or extracellular) solutions contained 10 mM HEPES, 2 mM EGTA, and specified concentrations of K^+ provided by KCl. The pH of all recording solutions was adjusted to 7.2 with methanesulfonate (MES). To maintain a constant ionic strength, the total concentration of sodium and potassium was maintained at 120 mM using NaOH. Excised patches were perfused with an intracellular solution containing 116 mM KOH, 4 mM KCl, 10 mM HEPES, 2 mM EGTA, supplemented with $CaCl_2$, $MgCl_2$, $SrCl_2$, or $BaCl_2$, pH adjusted to 7.2 with methanesulfonate (MES); the amount of $CaCl_2$ required to yield the concentration indicated was calculated according to the following stability constants (log *K*): Mg-EGTA, 5.28; Ca-EGTA, 10.86; Sr-EGTA, 8.43; and Ba-EGTA, 8.3 (Martell and Smith, 1974). The calculation included an adjustment for pH. Activation and blockade were measured by perfusing the intracellular face of the membrane patch with solutions containing different concentrations of divalent cations. All compounds for recording solution were obtained from Sigma (St. Louis, MO).

RESULTS

rSK2 channels show an inwardly rectifying I-V relationship at high $[Ca^{2+}]_i$

Fig. 1 *A* shows macroscopic current traces recorded from an excised inside-out patch containing rSK2 channels in symmetrical 120 mM K^+, whereas membrane voltage was linearly ramped from −100 to 100 mV. As the concentration of intracellular Ca^{2+} ($[Ca^{2+}]_i$) was raised from 0 to 5 μM, the ionic currents through rSK2 were increased with the half-maximum concentration of Ca^{2+} ($^{Ca}K_{1/2}$) at about 0.6

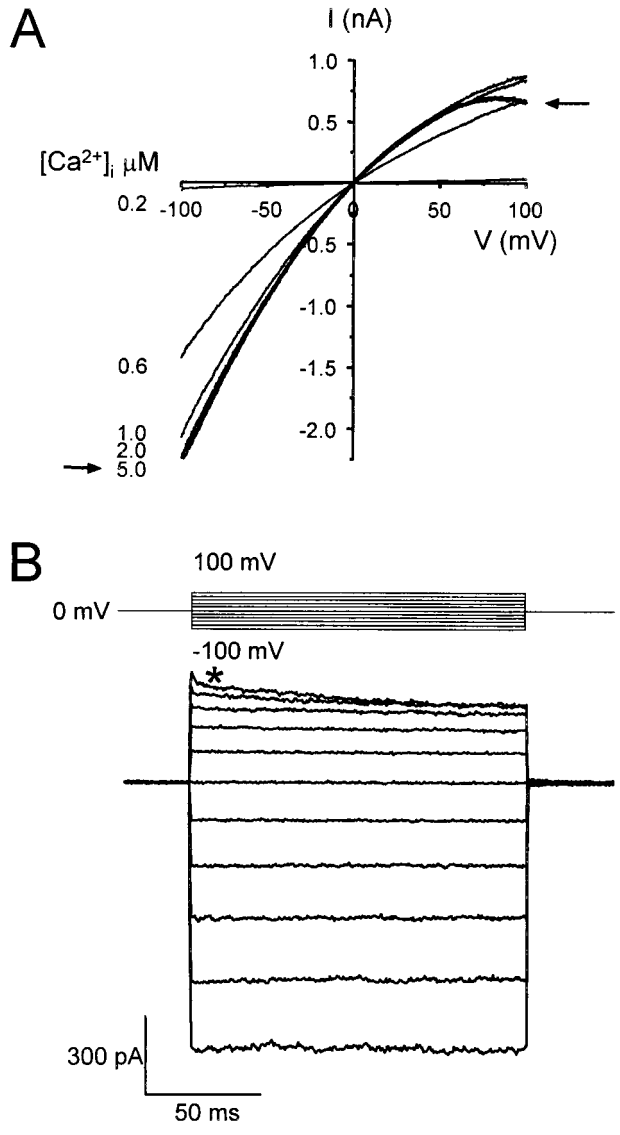

FIGURE 1 Macroscopic current-voltage relationship of rSK2 expressed in *Xenopus* oocytes. (*A*) Current traces elicited by 1 s voltage ramp from −100 mV to 100 mV of inside-out macropatches excised from oocytes expressing rSK2. Each current trace was averaged from three consecutive recordings obtained in the presence of the indicated concentrations of intracellular free Ca^{2+}. (*B*) Representative current traces evoked by voltage steps. In the presence of 2.0 μM $[Ca^{2+}]_i$, the membrane was stepped from holding voltage of 0 mV to 150 ms test potentials between −100 mV to 100 mV in 20 mV increments. Current relaxation observed at extreme positive voltages was indicated with an asterisk.

μM. At low $[Ca^{2+}]_i$ such as 0.2–0.6 μM, the I-V relationship of rSK2 showed only a slight inward rectification: the channel currents at a positive voltage are a little smaller than those at the identical negative voltage. However, the degree of rectification was dependent on $[Ca^{2+}]_i$ and was more profound at high $[Ca^{2+}]_i$. The inward rectification seems to be the result of the suppression of outward current at positive voltages. Due to such a strong reduction of the outward

current, the channel current evoked by 5 μM of $[Ca^{2+}]_i$ (indicated by an arrow) showed a negative conductance and became even smaller than the current evoked by 1 μM $[Ca^{2+}]_i$ at extreme positive voltages (Fig. 1 *A*). These results suggest that intracellular Ca^{2+} may block the channel in a voltage-dependent fashion. Fig. 1 *B* shows rSK2 currents evoked by voltage steps in the presence of 2.0 μM Ca^{2+} in the intracellular solution. When the membrane voltage was stepped from a holding potential of 0 mV to various negative test voltages, the rectangular current traces were recorded in a linear relationship with applied voltages. At positive voltage ranges, however, the steady-state current levels were much smaller than those expected for an ohmic response. The relaxation of ionic currents to lower levels observed at high voltage pulses (indicated by an asterisk) further supports the idea of voltage-dependent reduction of rSK2 at positive voltages by intracellular Ca^{2+}.

Activation of rSK2 channels by several intracellular divalent cations: Ba^{2+}, Sr^{2+}, Mg^{2+}, and Ca^{2+}

Because rSK2 currents were reduced by intracellular Ca^{2+} in a voltage-dependent manner and induced an inwardly rectifying I-V relationship, we investigated the effects of other alkaline earth metals, Mg^{2+}, Sr^{2+}, and Ba^{2+}, on the activation of the currents. The macroscopic rSK2 channel currents were activated with four different divalent cations and each current was normalized to the maximum inward current values in the presence of 5 μM intracellular Ca^{2+} (Fig. 2). Intracellular Sr^{2+} activated rSK2 currents with $^{Sr}K_{1/2}$ at 3.26 μM, and severe reductions of outward currents were observed in the positive membrane voltage range at concentrations >3 μM. The rSK2 channel currents were activated by intracellular Ba^{2+} in a much higher concentration range, $^{Ba}K_{1/2}$ of 43.3 μM, and the I-V relationship of the channel currents showed even stronger inward rectifications. In fact, no significant outward currents were observed throughout the activating concentration range, 10 to 100 μM, of Ba^{2+}. In Fig. 2 *B*, the current activation was measured at -90 mV where the effects of voltage-dependent blockade were minimal and were plotted against the concentration of each divalent cation tested. Whereas the channel currents were activated by submicromolar concentrations of intracellular Ca^{2+}, higher concentrations were need for Sr^{2+} and Ba^{2+}. In addition, the maximum current levels obtained for Sr^{2+} and Ba^{2+} were smaller, 0.92 and 0.42, respectively, than that of Ca^{2+} (Fig. 2 *B*). The maximum level of rSK2 currents activated by intracellular Ba^{2+} might be obscured by the rapid block occurring at high concentration even at -90 mV and thus slightly underestimated. The reduction of channel currents seen at 200 μM

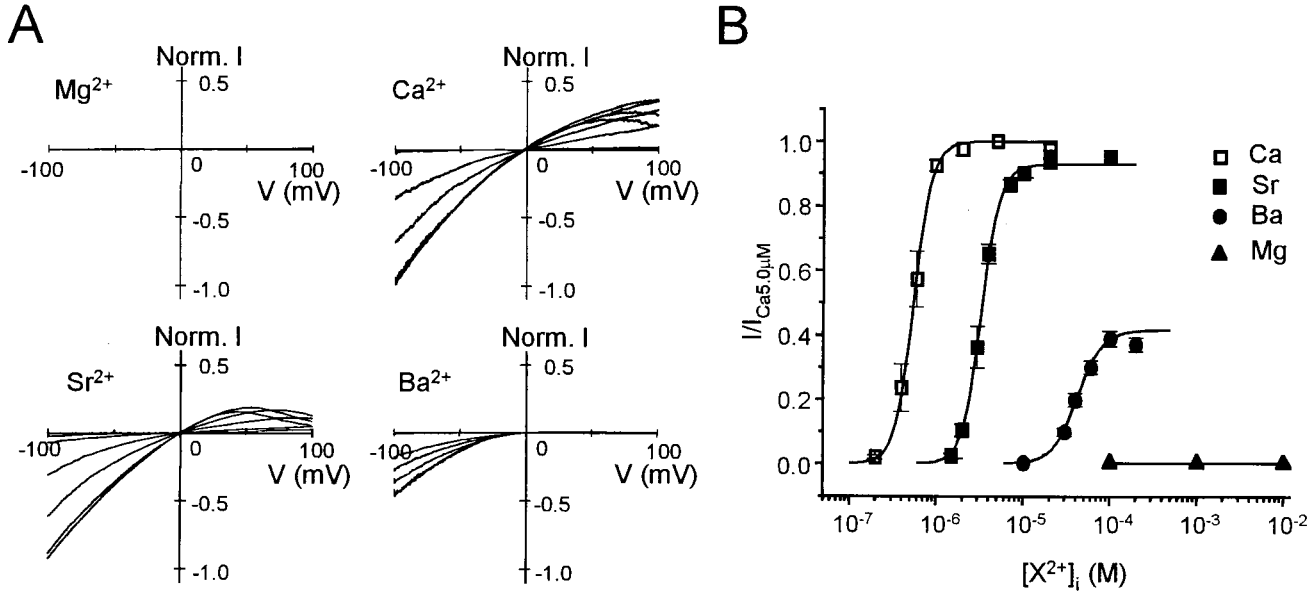

FIGURE 2 rSK2 channel activation by alkaline earth metals, Ba^{2+}, Sr^{2+}, Mg^{2+}, and Ca^{2+}. (*A*) Each current trace is normalized to maximum inward current value in the presence of 5 μM intracellular Ca^{2+}. Representative current traces are recorded in the presence of following concentrations of each divalent cation: 0.1, 1, and 10 mM of intracellular Mg^{2+}; 0, 0.2, 0.4, 0.6, 1, 2, 5, and 20 μM of Ca^{2+}; 1.5, 2, 3, 4, 10, and 20 μM of Sr^{2+}; and 10, 30, 40, 60, 100, and 200 μM of Ba^{2+}. (*B*) Fraction of activated currents ($I/I_{Ca5.0\ \mu M}$) obtained from the normalized current at -90mV were plotted against $[X^{2+}]_i$. The lines superimposed in the data correspond to least-squares fits using the Hill equation. The observed half activation constant of a divalent cation, X^{2+} ($^{X}K_{1/2}$) was estimated as 3.26 μM for Sr^{2+}, 43.29 μM for Ba^{2+}, and 0.55 μM for Ca^{2+}, respectively. The values of I_{max} were estimated as 0.92, 0.42, and 1 for Sr^{2+}, Ba^{2+}, and Ca^{2+}, respectively. The Hill coefficient values (n) of X^{2+} were 4.3, 3.2, and 4.1 for Sr^{2+}, Ba^{2+}, and Ca^{2+}, respectively. No measurable rSK2 channel currents were recorded in Mg^{2+} up to 10 mM.

Ba^{2+} might be the result of such blockade. In the case of Mg^{2+}, no measurable rSK2 currents were recorded even in the presence of 10 mM Mg^{2+}.

rSK2 channels were blocked by intracellular Mg^{2+} in a voltage-dependent manner

Because Mg^{2+} is present in cytoplasm at about a millimolar concentration (Birch, 1993) and fails to activate rSK2 channel, we examined whether intracellular Mg^{2+} affects the I-V relationship of rSK2 channel activated by Ca^{2+}. In the presence of 120 mM K^+ on both sides of the membrane and 0.6 μM $[Ca^{2+}]_i$ on the intracellular side to activate the channel, the addition of Mg^{2+} to the intracellular side

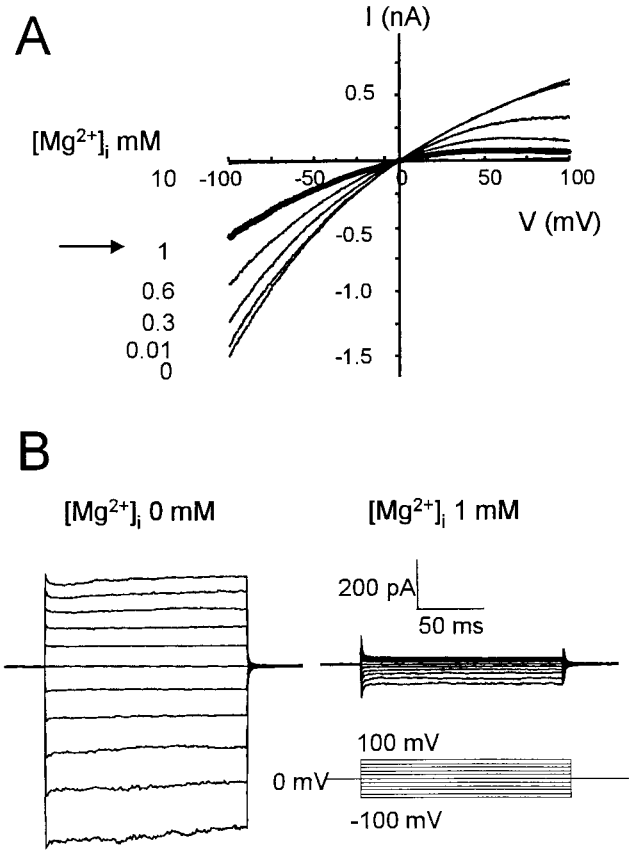

FIGURE 3 Intracellular Mg^{2+} reduces rSK2 channel currents in a concentration-dependent manner. (*A* and *B*) Macroscopic rSK2 currents were recorded in the presence of the indicated concentrations of intracellular Mg^{2+} and 0.6 μM $[Ca^{2+}]_i$. (*A*) Macroscopic rSK channel currents were recorded from excised patches by a 1-s voltage ramp from −100 mV to 100 mV in various concentrations of intracellular Mg^{2+}. The arrow indicates the I-V relationship obtained in the presence of 1 mM Mg^{2+}, which can be compared with the current blockade shown in (*B*). (*B*) Current traces recorded by voltage steps in the absence (*left*) and presence (*right*) of 1 mM intracellular Mg^{2+}. The currents were elicited in response to a voltage step from −100 mV to 100 mV in 20-mV increases from inside-out macropatches in the presence of 0.6 μM $[Ca^{2+}]_i$.

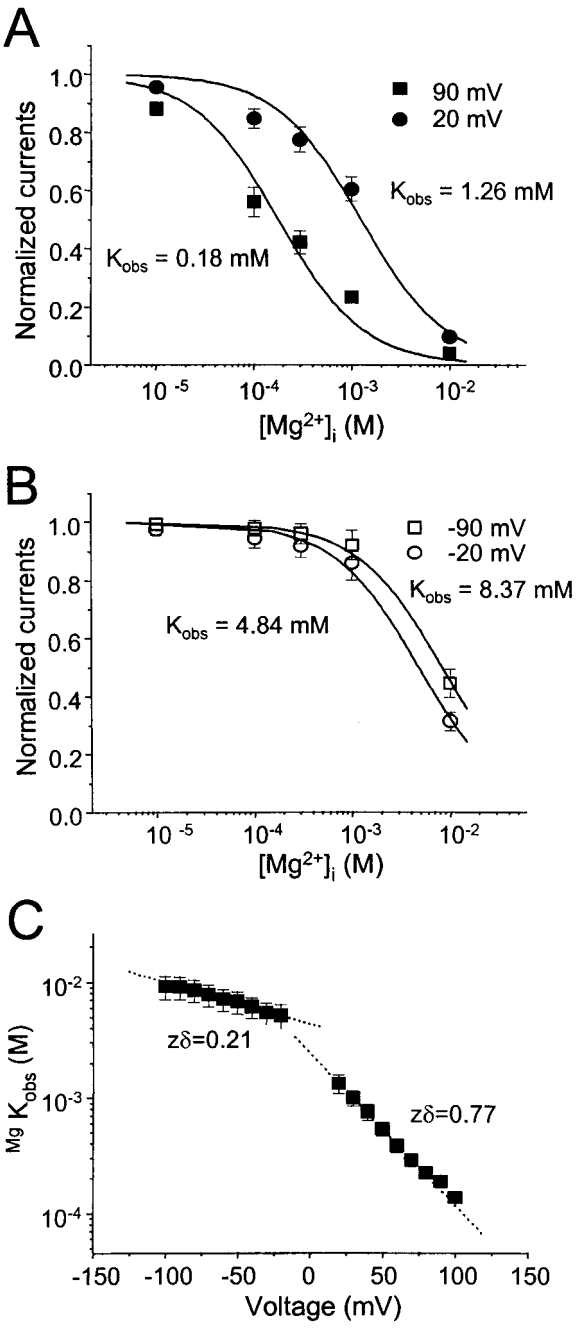

FIGURE 4 Voltage dependence of rSK2 channel blockade by intracellular Mg^{2+}. Fraction of unblocked currents (I/I_O) was plotted against $[Mg^{2+}]_i$ for two different membrane voltages in positive 90 mV and 20 mV (*A*) and negative −90 mV and −20 mV ranges (*B*). The lines superimposed on the data points correspond to least-squares fits using the Hill equation. The observed dissociation constants of Mg^{2+} ($^{Mg}K_{obs}$) were estimated as 0.18 mM at 90 mV, 1.26 mM at 20 mV, 4.84 mM at −20 mV, and 8.37 mM at −90 mV, respectively. (C) $^{Mg}K_{obs}$ were plotted against various membrane voltages. The lines superimposed on data correspond to least-squares fits using the Woodhull equation, $\ln{}^{Mg}K_{obs} = \ln{}^{Mg}K_{obs}(0\text{ mV}) - {}^{Mg}(z\delta)_{obs}FV/RT$. F, R, and T have their usual thermodynamic meaning.

caused a concentration-dependent reduction of rSK2 currents (Fig. 3, *A* and *B*).

We observed that the channel blockade by intracellular Mg^{2+} is highly voltage-dependent. Fig. 4, *A* and *B*, shows the fractions of unblocked currents at four representative membrane voltages plotted against the concentration of Mg^{2+} in the presence of 2 μM $[Ca^{2+}]_i$. Data points are fitted to the Hill equation for 1:1 binding and the observed dissociation constants for Mg^{2+} ($^{Mg}K_{obs}$) were determined (Fig. 4, *A* and *B*). As the membrane voltages were made more positive, the degree of current blockade was further increased, as if Mg^{2+} is driven into the channel by the positive membrane potential. Although the increase in membrane voltage by 70 mV resulted in about sevenfold increase in Mg^{2+} affinity under positive voltage ranges (Fig. 3 *A*), an identical voltage change gave less than twofold difference in negative voltages (Fig. 4 *B*). When we analyzed the dissociation constants ($^{Mg}K_{obs}$) at various voltages and plotted them against membrane voltage, we obtained two distinct slopes markedly different in positive and negative membrane voltages (Fig. 4 *C*). Using the Woodhull equation (Woodhull, 1973), the slopes, which are the empirical measurements of voltage dependence or $^{Mg}(z\delta)_{obs}$ values, were estimated as 0.21 for the negative voltage range and 0.77 for the positive range.

Intracellular Ca^{2+} reduced the affinity of internal Mg^{2+} for channel blockade

Because both Mg^{2+} and Ca^{2+} reduced rSK2 channel currents from intracellular side, we then examined how $[Ca^{2+}]_i$ affects the current blockade by internal Mg^{2+}. Fig. 5 *A* shows the current-voltage relationships at various concentrations of internal Mg^{2+} in the presence of 0.4 (raw trace not shown), 0.6, 2, and 20 μM of intracellular Ca^{2+}, re-

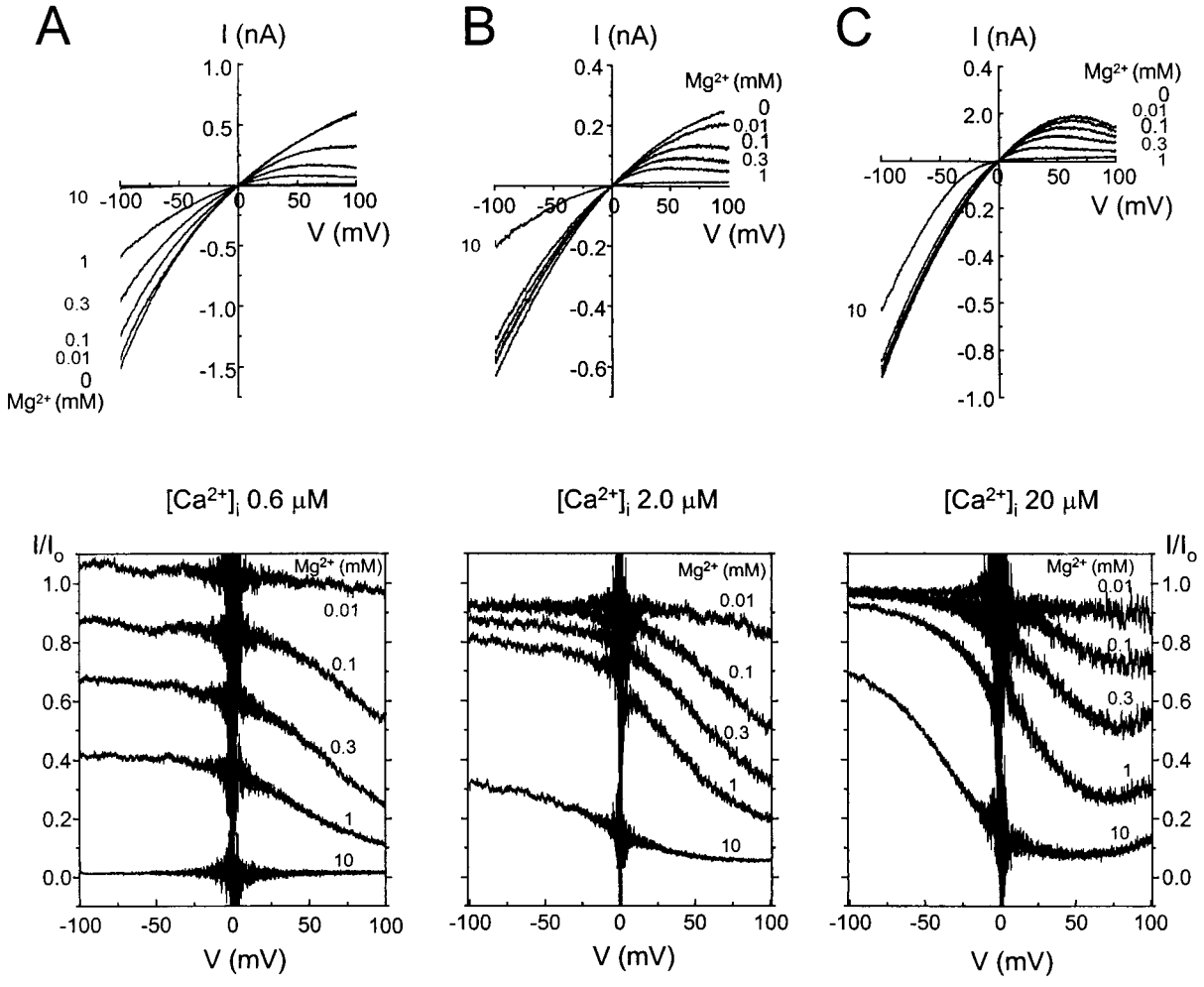

FIGURE 5 Effects of intracellular Ca^{2+} on the blockade of rSK current by intracellular Mg^{2+}. In the *upper* panels, representative macroscopic current traces of rSK2 channel were recorded at various $[Mg^{2+}]_i$ under symmetrical 120 mM K^+ in the presence of 0.6 μM (*A*), 2 μM (*B*), and 20 μM $[Ca^{2+}]_i$ (*C*), respectively. The fraction of unblocked currents (I/I_O) was plotted against membrane voltage from the trace obtained (*lower* panels). The concentration of intracellular Ca^{2+} and Mg^{2+} were as indicated.

spectively. As $[Ca^{2+}]_i$ was increased from 0.4 to 20 μM, a significant reduction of outward currents was observed even in the absence of internal Mg^{2+} (top traces shown in the upper panels of Fig. 5, *A* and *C*). The I-V relationship was further rectified by the titration using intracellular Mg^{2+}. At all four $[Ca^{2+}]_i$ tested, the reduction of channel currents were voltage-dependent as shown in the lower panels of Fig. 5. When the fraction of unblocked currents (I/I_0) is plotted against membrane voltage, however, it was noticed that the affinity of internal Mg^{2+} was decreased as the concentration of intracellular Ca^{2+} increased from 0.6 μM to 20 μM (Fig. 5, lower panels). The relief of blockade observed at extreme positive voltages at 20 μM of internal Ca^{2+} (Fig. 5 *C*, lower panel) seems to be due to the strong inward rectification of currents caused by high Ca^{2+}. To compare the blockade of four intracellular Ca^{2+} concentrations, we plotted the fraction of unblocked currents (I/I_o) of the rSK2 channel at -90 mV and 90 mV against various intracellular Mg^{2+} and fitted the data with Hill functions in Fig. 6. As we increased $[Ca^{2+}]_i$ from 0.4 μM to 20 μM, the observed dissociation constants ($^{Mg}K_{obs}$) were increased from 0.13 mM to 0.55 mM at 90 mV (Fig. 6 *A*) and 0.42 mM to 23.5 mM at -90 mV (Fig. 6 *B*). Only a small change in Mg^{2+} affinity was seen at low concentration of $[Ca^{2+}]_i$, for example, 0.13 mM and 0.18 mM of $^{Mg}K_{obs}$ at 0.4 μM and 2 μM of $[Ca^{2+}]_i$ at 90 mV. Since rSK2 channel is activated dramatically in this concentration range of Ca^{2+} (from about 20% to the maximal current level with $^{Ca}K_{1/2}$ of 0.6 μM and n of 4.1; Fig. 2 *B*), this result strongly suggests that Mg^{2+} binds to both closed and open rSK2 channels with a similar affinity. Thus, the decreased binding affinities of Mg^{2+} at higher $[Ca^{2+}]_i$ are likely due to the interference by intracellular Ca^{2+}.

External K^+ alters the affinity and voltage dependence of intracellular Mg^{2+} blockade

We next examined how the concentration of external K^+ ($[K^+]_e$) affects the channel blockade by internal Mg^{2+}. It was discovered that the apparent affinity of intracellular blocking ions that cause rectification also depends on the concentration of extracellular K^+ in several different K^+ channels (Armstrong and Binstock, 1965; Bezanilla and Armstrong, 1972; Hille, 1975). This phenomenon is commonly referred to as *trans* knockoff of blocking ions by extracellular K^+ and used as an evidence for the blocking of conduction pore by a specific channel inhibitor. Fig. 7 *A* shows the representative current traces in the presence of 4 mM of $[K^+]_e$. The fractions of unblocked currents (I/I_0) obtained from Fig. 7 *A* were plotted against $[Mg^{2+}]_i$ for 10 mV of membrane voltage in Fig. 7 *B*. The apparent affinity of Mg^{2+} was increased as the external K^+ concentration was decreased. By lowering the external K^+ concentration from 120 mM to 4 mM, the apparent affinity for Mg^{2+} increased from 1.4 mM to 0.5 mM at 10 mV (Fig. 7 *B*). Thus, this also supports the fact that Mg^{2+} blocks the channel current by binding in the ion conduction pore of rSK2 channels where internal Mg^{2+} can be destabilized by extracellular K^+. We also observed a decrease in voltage dependency (δ) due to internal Mg^{2+} blockade from 0.39

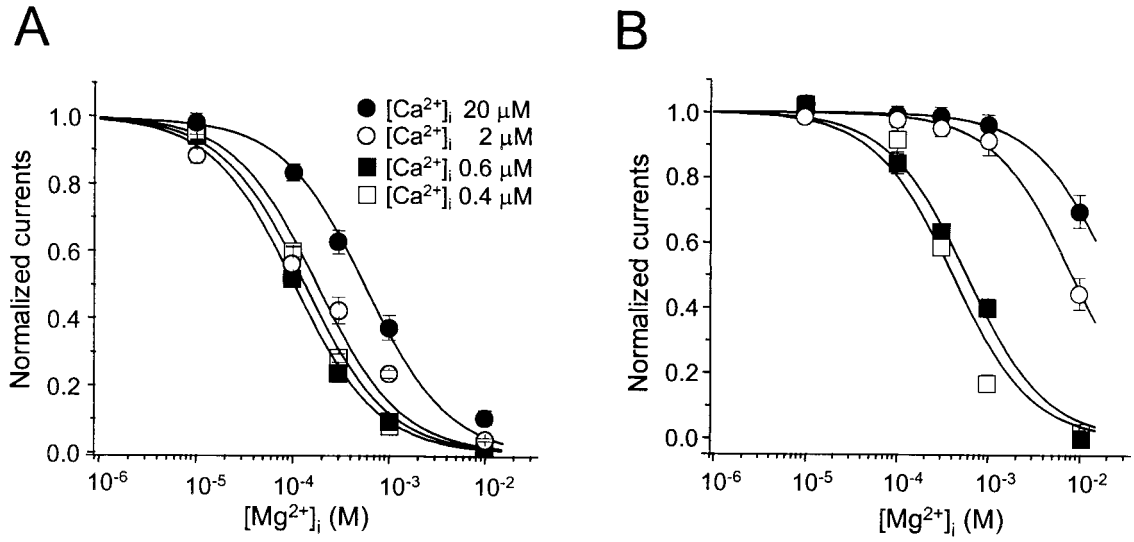

FIGURE 6 Intracellular Ca^{2+} decreases the binding affinity of Mg^{2+} for rSK in a voltage-dependent manner. Fraction of unblocked currents (I/I_O) obtained at two different membrane voltages, 90mV (*A*) and -90 mV (*B*), were plotted against various $[Mg^{2+}]_i$. The concentration of intracellular Ca^{2+} was as indicated. The lines superimposed on the data correspond to least-squares fits using the Hill equation. The observed dissociation constants of Mg^{2+} ($^{Mg}K_{obs}$) were estimated as 0.13 mM for 0.4 μM $[Ca^{2+}]_i$, 0.10 mM for 0.6 μM $[Ca^{2+}]_i$, 0.18 mM for 2 μM $[Ca^{2+}]_i$, and 0.55 mM for 20 μM $[Ca^{2+}]_i$ at 90 mV, and 0.42 mM for 0.4 μM $[Ca^{2+}]_i$, 0.58 mM for 0.6 μM $[Ca^{2+}]_i$, 8.37 mM for 2 μM $[Ca^{2+}]_i$, and 23.5 mM for 20 μM $[Ca^{2+}]_i$ at -90 mV, respectively.

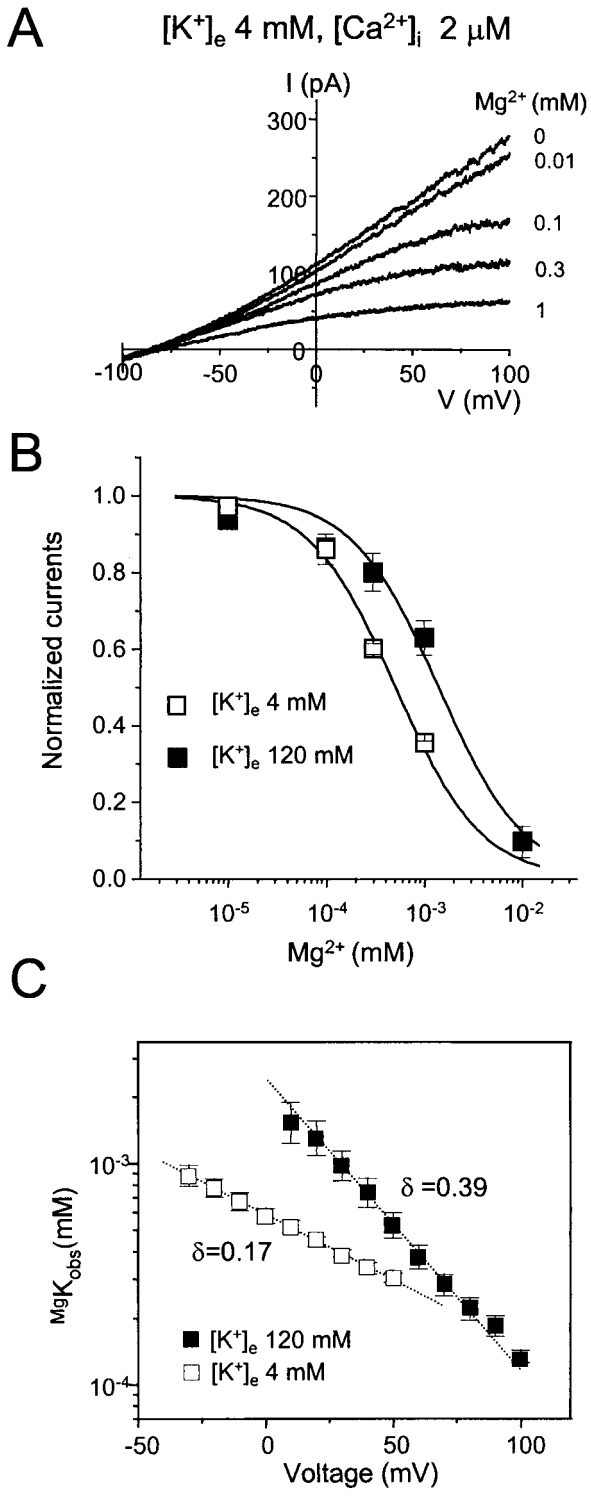

FIGURE 7 Voltage and extracellular K^+ dependence of rSK2 channel blockade by intracellular Mg^{2+}. (*A*) Representative macroscopic currents recorded with 4 mM of extracellular K^+ concentration in the presence of various $[Mg^{2+}]_i$. Intracellular concentration of K^+, $[K^+]_i$, was 120 mM. (*B*) Fraction of unblocked currents (I/I_0) measured at 10 mV was plotted against $[Mg^{2+}]_i$. The lines superimposed on the data correspond to least-squares fits using the Hill equation. $^{Mg}K_{obs}$ values were estimated as 0.5 mM for 4 mM of extracellular K^+ concentration, $[K^+]_e$, and 1.4 mM for 120 mM $[K^+]_e$, respectively. (*C*) $^{Mg}K_{obs}$ values were plotted against various membrane voltages at two different extracellular K^+ concentrations, 4 mM and 120 mM. The lines superimposed on data correspond to least-squares fits using the Woodhull equation, $\ln^{Mg}K_{obs} = \ln^{Mg}K_{obs}(0\ mV) - {}^{Mg}(z\delta)_{obs}FV/RT$.

to 0.17 as extracellular K^+ concentration was lowered (Fig. 7 *C*).

In a recent study, the mechanism of such extracellular K^+ dependence was studied for inwardly rectifying K^+ channels (Spassova and Lu, 1998). In the case of ROMK1, both the affinity and the voltage dependence of the blocking ions such as quaternary ammoniums or Mg^{2+} are varied as a function of extracellular K^+. Spassova and Lu (1998) proposed that the voltage-dependent channel blockade resulted, at least in part, from the energetic coupling between the blocking ion and permeating K^+. To verify whether the dependence of external K^+ observed in rSK2 channels is due to a similar mechanism, we quantified the effects of external K^+ on internal Mg^{2+} blockade at various membrane voltages. We first determined $^{Mg}K_{obs}(0\ mV)$, the observed equilibrium dissociation constant for Mg^{2+} at 0 mV, and $^{Mg}(z\delta)_{obs}$, which measures the voltage dependence of Mg^{2+} binding, at various $[K^+]_e$. As shown in Fig. 8 *A*, $^{Mg}K_{obs}(0\ mV)$ increases linearly with increase in $[K^+]_e$ as if the internal Mg^{2+} and external K^+ compete for the pore (see Discussion). Moreover, $^{Mg}(z\delta)_{obs}$ increased with $[K^+]_e$ in a saturating manner, $^{Mg}(z\delta)_{obs}$ at infinite $[K^+]_e$ of 1.01 and the apparent dissociation constant for the binding of external K^+ to the pore of about 70 mM (Fig. 8 *B*). These results further support the idea that the permeant ion, K^+, interacts with Mg^{2+} within the conduction pathway of rSK2 channels, and both the apparent affinity and the voltage dependence observed in intracellular Mg^{2+} blockade are, at least in part, due to the coupling between Mg^{2+} and K^+.

DISCUSSION

In this study, we investigated the effects of intracellular divalent cations on small-conductance Ca^{2+}-activated K^+ channels expressed in *Xenopus* oocytes. Divalent cations such as Ca^{2+}, Sr^{2+}, and Ba^{2+} not only activate rSK2 channel but also block the channel currents in a voltage-dependent manner and, thus, rectify the I-V relationship of the channel to an inward direction. The rank order for activation of rSK2 channels obtained this study, $Ca^{2+} > Sr^{2+} > Ba^{2+}$, agrees well with the sequence of metal ion selectivity for formation of the calmodulin-metal-target peptide ternary complex using surface plasmon resonance spectroscopy (Ozawa et al., 1999). Because rSK2 channel currents activated by intracellular Ba^{2+} were also inhibited under a similar concentration range, the Ba^{2+}-activated rSK2 currents above 100 μM may not represent faithfully the maximum currents even at -90 mV, where the effects of channel blockade is minimal (Fig. 2). Thus, the half-

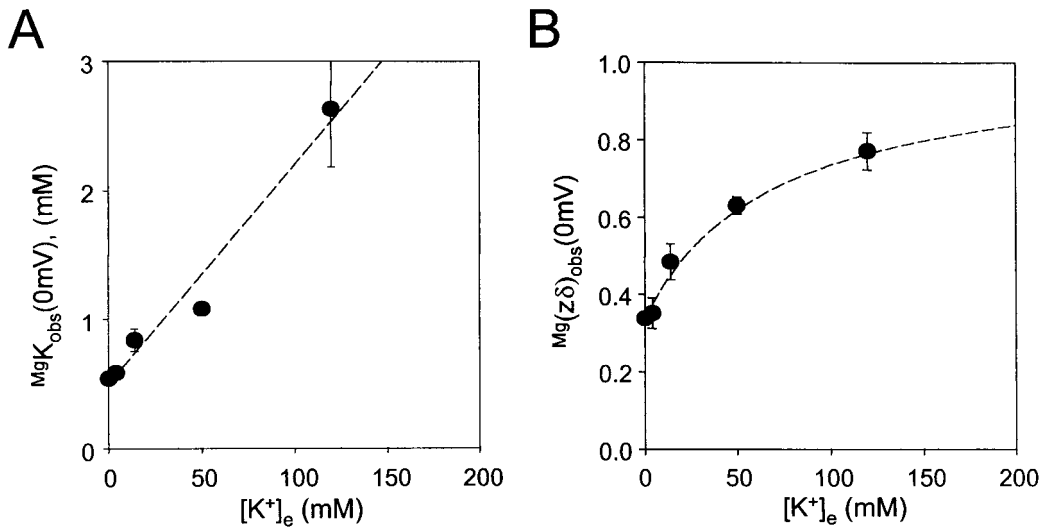

FIGURE 8 Summary of extracellular K^+ dependence of rSK2 channel blockade by internal Mg^{2+}. (*A*) The dissociation constant of Mg^{2+} estimated at 0 mV, ^{Mg}K(0 mV), was plotted against $[K^+]_e$. The dashed line corresponds to the least-squares fit of linear equation $^{Mg}K(0\ mV) = 0.513 + 0.017\ [K^+]_e$. (*B*) $^{Mg}(z\delta)_{obs}$ was plotted against $[K^+]_e$. The curve corresponds to the least-square fit by the equation $^{Mg}(z\delta)_{obs} = \{(^{Mg}(z\delta)_{inf} - {}^{Mg}(z\delta)_0)\ [K^+]_e\}/([K^+]_e + {}^{K}K_{obs}) + {}^{Mg}(z\delta)_0$, where $^{K}K_{obs}$ is the apparent dissociation constant for the binding of external K^+ to the pore, whereas $^{Mg}(z\delta)_0$ and $^{Mg}(z\delta)_{inf}$ are $^{Mg}(z\delta)_{obs}$ when concentrations of extracellular K^+ ($[K^+]_e$) are zero and infinity, respectively. This fit gives $^{Mg}(z\delta)_{inf} = 1.01$ and $^{K}K_{obs} = 0.07$ M.

activation constant and the Hill coefficient of Ba^{2+} may be significantly underestimated. These results are also consistent with a previous study on the activation of human intermediate-conductance Ca^{2+}-activated K^+ channel, hIK1 (Cao and Houamed, 1999). Although it failed to activate rSK2 channel, Mg^{2+}, the most abundant physiological divalent cation within the cell, also reduced the rSK2 channel in a voltage-dependent manner and further rectified the I-V relationship of rSK2 channel activated by Ca^{2+}.

The overall effect of intracellular Mg^{2+} on rSK2 channel current is consistent with the idea that the divalent cation directly binds to channel conduction pore and blocks the K^+ permeation for several reasons. Magnesium ion reduces rSK2 currents in a voltage-dependent manner and the reduction of macroscopic currents can be fit reasonably well with the Hill equation of single binding (Fig. 4, *A* and *B*). Secondly, the affinity and the voltage dependence of intracellular Mg^{2+} for rSK2 channel are altered by the concentration of extracellular K^+ (Figs. 7 and 8). We also found that the Mg^{2+} blockade is independent of the open channel probability of rSK2 channel (Fig. 6) and intracellular divalent cations compete each other for the blocking site.

Although the membrane topology and the gating mechanism are quite different, SK_{Ca} channels containing six-transmembrane domains seem to have similar underlying mechanism for inwardly rectifying I-V relationship compared with K_{ir} channels, the two-transmembrane K^+ channels. The dependence of extracellular K^+ observed for an inward rectifier K^+ channel, ROMK1, was explained by the coupled movement of K^+ and internal blocking ions, such as Mg^{2+} (Spassova and Lu, 1998). Based on a two-site single vacancy model, Spassova and Lu (1998) described that the linear relationship between the apparent affinity of a blocker, tetraethylammonium, and the concentration of extracellular K^+ satisfied the coupled movement of these ions. The apparent affinity of internal Mg^{2+} for SK2 channels also showed a linear correlation with extracellular K^+ (Fig. 8 *A*), strongly supporting the idea that a similar mechanism underlies the inwardly rectifying I-V relationship caused by intracellular Mg^{2+}. It is also intriguing to find that the apparent voltage dependence of the Mg^{2+} blockade, $^{Mg}(z\delta)_{obs}$, shows a saturating relationship with the increased extracellular K^+ just as found in the blockade of ROMK1 by quaternary ammoniums or Mg^{2+}. Although the observed affinity for Mg^{2+} of rSK2 was about fivefold higher than that of ROMK1, the observed voltage dependence, $z\delta_{obs}$, of the two channels were comparable (Spassova and Lu, 1998). It is also worth considering the mechanistic interpretation of the two markedly different $(z\delta)_{obs}$ values of Mg^{2+} blockade observed under a symmetrical K^+ condition (Fig. 4 *C*). A sharp contrast in $(z\delta)_{obs}$ values found in the positive and the negative voltage ranges can result from the differences in the K^+-affinity to the channel pore occupied and unoccupied by other cations such as Mg^{2+} or K^+, since the transmembrane voltage could influence the occupancy and, thus, the coupling among those cations. Although we focused our detailed experiments on rSK2 channel in this study, similar blockades by intracellular divalent cations were also observed in other subclasses of SK channels and even in an intermediate-conductance Ca^{2+}-activated K^+ channel (H. Soh and C.-S. Park, unpublished observations).

Considering the physiological functions of SK_{Ca} channels in excitable cells, it is intriguing to find that these channels exhibit strong inward rectification in I-V relationship under physiologically relevant concentrations of intracellular divalent cations. At the intracellular concentrations of 20 μM Ca^{2+} and 1 mM Mg^{2+} (such as shown in Fig. 5 *C*, upper panel), the I-V relationship of rSK2 channel is similar to that of strong inward rectifier K^+ channels recorded under symmetrical K^+ concentration (Lu and MacKinnon, 1994). Since the local concentration of intracellular Ca^{2+} is known to increase up to tens of micromolars during the action potential (Regehr and Tank, 1992), the I-V relationship of SK_{Ca} should be altered or can be modulated by the intracellular Ca^{2+}. Since the characteristic I-V relationship allows inward rectifier K^+ channels to regulate the resting membrane potentials without impeding the generation of action potentials, SK_{Ca} channels, as Ca^{2+}-activated inward rectifier K^+ channels, may be suited for their roles in repolarizing the membrane potentials for repetitive action potentials upon the increase in $[Ca^{2+}]_i$. Therefore, intracellular Ca^{2+} acts as a dynamic modulator of channel permeation as well as the direct activator of channel gating for small conductance Ca^{2+}-activated K^+ channels.

We thank Dr. John P. Adelman (The Vollum Institute, Oregon Health Sciences University, Portland, OR) for providing us rSK2 cDNA. We also thank Dr. C. Miller (Brandeis University, Waltham, MA) for his valuable comments, and to the other members of Neuro-Biochemistry Laboratory at K-JIST for their timely help throughout the work. This research was supported by grants from the Ministry of Science and Technology of Korea (Star Project 98-NQ-07–01-A), and the Korea Research Foundation (1998–001-F00130 and BK21).

REFERENCES

Armstrong, C. M., and L. Binstock. 1965. Anomalous rectification in the squid giant axon injected with tetraethylammonium. *J. Gen. Physiol.* 48:859–872.

Birch, N. J. 1993. The effects of magnesium on excitable tissues. *In* Magnesium and the Cell. C. H. Fry and A. B. Proctor, editors. Academic Press, San Diego, CA. 217–234.

Bezanilla, F., and C. M. Armstrong. 1972. Negative conductance caused by entry of sodium and cesium ions into the potassium channels of squid axons. *J. Gen. Physiol.* 60:588–608.

Cao, Y., and K. M. Houamed. 1999. Activation of recombinant human SK4 channels by metal cations. *FEBS Lett.* 446:137–141.

Doupnik, C. A., N. Davidson, and H. A. Lester. 1995. The inward rectifier potassium channel family. *Curr. Opin. Neurobiol.* 5:268–277.

Ha, T. S., S. Y. Jeong, S. W. Cho, H. K. Jeon, G. S. Roh, W. S. Choi, and C. S. Park. 2000. Functional characteristics of two BK_{Ca} channel variants differentially expressed in rat brain tissues. *Eur. J. Biochem.* 267: 910–918.

Hille, B. 1975. Ionic selectivity of Na and K channels of nerve membranes. *Membranes.* 3:255–323.

Hille, B. 1992. Ionic Channels of Excitable Membranes. Sinauer, Sunderland, MA.

Ishii, T. M., J. Maylie, and J. P. Adelman. 1997. Determinants of apamin and curarine block in SK potassium channels. *J. Biol. Chem.* 272: 23195–23200.

Keen, J. E., R. Kawaled, D. L. Farrens, T. Neelands, A. Rivard, C. T. Bond, A. Janowsky, B. Fakler, J. P. Adelman, and J. Maylie. 1999. Domains responsible for constitutive and Ca^{2+}-dependent interactions between calmodulin and small conductance Ca^{2+}-activated potassium channels. *J. Neurosci.* 19:8830–8838.

Kohler, M., B. Hirschberg, C. T. Bond, J. M. Kinzie, N. V. Marrion, J. Maylie, and J. P. Adelman. 1996. Small-conductance, calcium-activated potassium channels form mammalian brain. *Science.* 273:1709–1714.

Lancaster, B., R. A. N. Nicoll, and D. J. Perkel. 1991. Calcium activated two types of potassium channels in rat hippocampal neuron in culture. *J. Neurosci.* 11:23–30.

Liman, E. R., J. Tytgat, and P. Hess. 1992. Subunit stoichiometry of a mammalian K^+ channel determined by construction of multimeric cDNAs. *Neuron.* 9:861–871.

Lu, Z., and R. MacKinnon. 1994. Electrostatic tuning of Mg^{2+} affinity in an inward-rectifier K^+ channel. *Nature.* 371:243–245.

Martell, A. E., and R. M. Smith. 1974. Critical Stability Constants, Vol. 1. Plenum, New York.

Ozawa, T., K. Sasaki, and Y. Umezawa. 1999. Metal ion selectivity for formation of the calmodulin-metal-target peptide ternary complex studied by surface plasmon resonance spectroscopy. *Biochim. Biophys. Acta.* 12:1434.(2):211–220

Park, C. S., and R. MacKinnon. 1995. Divalent cation selectivity in a cyclic nucleotide-gated ion channel. *Biochemistry.* 34:13328–13333.

Regehr, W. G., and D. W. Tank. 1992. Calcium concentration dynamics produced by synaptic activation of CA1 hippocampal pyramidal cells. *J. Neurosci.* 12:4202–4023.

Spassova, M., and Z. Lu. 1998. Coupled ion movement underlies rectification in an inward-rectifier K^+ channel. *J. Gen. Physiol.* 112:211–221.

Vergara, C., R. Latorre, N. V. Marrion, and J. P. Adelman. 1998. Calcium-activated potassium channels. *Curr. Opin. Neurobiol.* 8:321–329.

Woodhull, A. M. 1973. Ionic blockage of sodium channels in nerve. *J. Gen. Physiol.* 61:687–708.

Xia, X. -M., B. Fakler, A. Rivard, G. Wayman, T. Johnson-Pais, J. E. Keen, T. Ishii, B. Hirschberg, C. T. Bond, S. Lutsenko, J. Maylie, and J. P. Adelman. 1998. Mechanism of calcium gating in small-conductance calcium-activated potassuim channels. *Nature.* 395:503–507.